

Relation between oxygen activity gradient in the internal oxidation zone of Mn alloyed steel and the composition of oxide precipitates

Mao, William; Sloof, Willem G.

DOI

[10.1016/j.scriptamat.2017.03.009](https://doi.org/10.1016/j.scriptamat.2017.03.009)

Publication date

2017

Document Version

Final published version

Published in

Scripta Materialia

Citation (APA)

Mao, W., & Sloof, W. G. (2017). Relation between oxygen activity gradient in the internal oxidation zone of Mn alloyed steel and the composition of oxide precipitates. *Scripta Materialia*, 135, 29-32.
<https://doi.org/10.1016/j.scriptamat.2017.03.009>

Important note

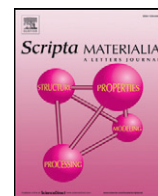
To cite this publication, please use the final published version (if applicable).
Please check the document version above.

Copyright

Other than for strictly personal use, it is not permitted to download, forward or distribute the text or part of it, without the consent of the author(s) and/or copyright holder(s), unless the work is under an open content license such as Creative Commons.

Takedown policy

Please contact us and provide details if you believe this document breaches copyrights.
We will remove access to the work immediately and investigate your claim.



Regular Article

Relation between oxygen activity gradient in the internal oxidation zone of Mn alloyed steel and the composition of oxide precipitates

Weichen Mao^{a,b,*}, Willem G. Sloof^a^a Department of Materials Science and Engineering, Delft University of Technology, Mekelweg 2, 2628 CD, Delft, The Netherlands^b Materials innovation institute (M2i), Elektronikaweg 25, 2628 XG, Delft, The Netherlands

ARTICLE INFO

Article history:

Received 19 January 2017

Accepted 8 March 2017

Available online 26 March 2017

Keywords:

Mn alloyed steel

Internal oxidation

(Mn_{1-x}Fe_x)O mixed oxide

Composition depth profile

Local thermodynamic equilibrium

ABSTRACT

An internal oxidation zone with (Mn_{1-x}Fe_x)O mixed oxide precipitates occurs after annealing a Fe – 1.7 at.% Mn steel at 950 °C in N₂ plus 5 vol% H₂ gas mixture with dew point of 10 °C. Local thermodynamic equilibrium in the internal oxidation zone is established during annealing of the Mn alloyed steel. As a result, the composition of (Mn_{1-x}Fe_x)O precipitates depends on the local oxygen activity. The oxygen activity decreases as a function of depth below steel surface, and consequently the concentration of Fe decreases in the (Mn_{1-x}Fe_x)O precipitates.

© 2017 Acta Materialia Inc. Published by Elsevier Ltd. All rights reserved.

Mn is one of the major alloying elements in advanced high strength steels, which are used for automotive applications to reduce the weight of car bodies and thereby reducing fuel consumption and CO₂ emissions. To protect these steels against corrosion a zinc coating is applied, usually by hot-dip galvanizing. However, during annealing of these steels prior to galvanizing the Mn can be oxidized easily, which may impair the zinc coating adhesion [1]. Then, it is beneficial if the oxides are formed beneath rather than at the steel surface.

The kinetics of internal oxidation of Fe–Mn binary steel alloys has been studied experimentally [2] and a numerical model has been developed to simulate the internal oxidation behaviour of Fe–Mn binary alloys [2,3]. Extension of this model to simulate internal oxidation of multi-element alloyed steels has also been reported [3,4]. A vital assumption in all internal oxidation models [2,3,5], as in the model adopted here [2], is that local thermodynamic equilibrium is reached between dissolved oxygen, alloying elements, iron matrix and oxide precipitates. However, experimental proof for the establishment of local thermodynamic equilibrium inside alloy matrix during internal oxidation of Mn alloyed steels is lacking. In this work, it will be shown from the observed composition depth profile of the internal oxide precipitates formed during internal oxidation of Mn alloyed steel that local thermodynamic equilibrium indeed occurs.

FeO and MnO, which are known as Wüstite and manganosite respectively, have the same rock salt crystal structure. Hence, FeO and

MnO can form a continuous solid solution also known as manganowüstite, henceforth denoted as (Mn_{1-x}Fe_x)O; see e.g. [6]. When annealing steels alloyed with Mn, (Mn_{1-x}Fe_x)O mixed oxide can be formed at the steel surface even below the dissociation oxygen partial pressure of FeO [7]. The concentration of Fe-ions dissolved in the external (Mn_{1-x}Fe_x)O increases with dew point (i.e. oxygen partial pressure) in the annealing atmosphere [7]. When these Mn steel alloys are oxidized internally, (Mn_{1-x}Fe_x)O precipitates are formed in the internal oxidation zone (IOZ). However, the composition of these precipitates depends on the local activity (i.e. chemical potential) of dissolved oxygen. Upon internal oxidation a gradient of oxygen activity in the IOZ exists which results in the inward diffusion of dissolved oxygen. Hence, if local thermodynamic equilibrium between dissolved oxygen and oxide precipitates is established, it is expected that the concentration of Fe in the (Mn_{1-x}Fe_x)O decreases with depth.

In this work, the concentration and activity depth profiles of dissolved oxygen are predicted quantitatively for steels alloyed with Mn using a numerical internal-oxidation simulation tool [2]. Since the thermodynamic data of the Fe–Mn–O ternary system have been well assessed in the currently available thermodynamic databases [8], the corresponding composition of the internal (Mn_{1-x}Fe_x)O as a function of depth is calculated using a thermodynamic computation tool [9]. The actual composition depth profile of the internal oxide precipitates is determined experimentally from their lattice parameter as obtained from X-ray diffractometry (XRD).

The steel alloyed with 1.7 at.% Mn were annealed for 1 h at 950 °C in N₂ + 5 vol% H₂ gas mixture at a dew point of 10 °C, corresponding with an oxygen partial pressure of 2.3×10^{-17} . This dew point was realized

* Corresponding author at: Department of Materials Science and Engineering, Delft University of Technology, Mekelweg 2, 2628 CD, Delft, The Netherlands.

E-mail address: w.mao@tudelft.nl (W. Mao).

by adding de-aerated and deionized water vapour to the gas flow of 1500 sccm passing through a 30 mm inner diameter quartz tube in a horizontal furnace (Carbolite MTF 12/38/850, UK). Based on the fluctuation of the dew point during annealing observed with a cooled mirror analyzer (Optidew, Michell Instruments, UK), the uncertainty of the dew point in the annealing atmosphere is about 2 °C. The annealing process is terminated by moving the steel sample to the cold zone of the quartz tube, allowing the steel sample to be cooled down to room temperature. The cooling rate from the annealing temperature to about 400 °C is about 180 °C/min. Further details of the experimental setup are described elsewhere [2]. Under these annealing conditions internal oxidation of Mn alloyed steel will prevail [10]. The composition of the steel used is: 0.48 at.% C, 1.72 at.% Mn, 0.097 at.% Si, 0.004 at.% Al and balance Fe.

To obtain the composition depth profile of internal $(\text{Mn}_{1-x}\text{Fe}_x)\text{O}$ with X-ray diffractometry (XRD), the surface of sample after annealing was mechanically polished to remove a layer with certain thickness. The polishing was done with 1 μm diamond grains using a soft cloth (Lam Plan MM431, UK). After each polishing step the sample was thoroughly cleaned ultrasonically with isopropanol. The thickness of the surface layer removed was determined from the measured weight loss of the sample after polishing and considering the polished surface area. For the density of the steel 7.87 g/cm^3 is taken. The sample was weighted with an analytical balance (Mettler M55A, Switzerland) having an accuracy of $\pm 10 \mu\text{g}$.

After each polishing step, the lattice constant of the $(\text{Mn}_{1-x}\text{Fe}_x)\text{O}$ precipitates in the alloy matrix was determined from XRD measurements. XRD patterns were recorded with a Bruker D8 Discover diffractometer in the grazing incidence geometry using $\text{Co K}\alpha$ radiation, in the 2θ region between 37° and 57° with a step size of 0.01° 2θ and a dwell time of 30 s. The incidence angle of the X-ray beam was fixed at 3° with respect to the sample surface. As the analysis depth, the depth below the surface corresponding with 70% of the diffracted intensity of pure iron was taken, which is 1.27 to 1.34 μm [11] for 2θ from 30° to 60°. The data evaluation was done with the Bruker software Diffrac.EVA version 4.0. The position of the (111) and (200) diffraction lines of $(\text{Mn}_{1-x}\text{Fe}_x)\text{O}$ was determined by fitting a parabola to the top of the diffracted intensity peak after smoothing and stripping $\text{K}\alpha_2$ contribution [12]. The peak positions were corrected for instrumental errors by measuring reference SRM LaB₆ 660 [13] on a (510)-Si wafer using the same acquisition parameters as used for the sample, except that the dwell time per step was 1 s.

The (111) and (200) peak positions determined of the $(\text{Mn}_{1-x}\text{Fe}_x)\text{O}$ precipitates were also corrected for any residual stress, as determined by the so-called $\sin^2\psi$ -method [11].

The composition of $(\text{Mn}_{1-x}\text{Fe}_x)\text{O}$ formed in a Fe-Mn binary alloy in thermodynamic equilibrium with a gaseous oxidizing environment as a function of oxygen partial pressure at 850, 950 and 1050 °C is presented in Fig. 1(a). This diagram was calculated using Factsage [9] by considering thermodynamic equilibrium between a Fe-Mn alloy, $(\text{Mn}_{1-x}\text{Fe}_x)\text{O}$ and a gas mixture of Ar + O₂ at atmospheric pressure. First, the thermodynamic data for the solid solution oxide $(\text{Mn}_{1-x}\text{Fe}_x)\text{O}$ was taken from the FToxid database [8]. Then, a gas mixture of Ar and O₂ with a total pressure of 1 atm at different oxygen partial pressures was created with thermodynamic data from the FactPS database [8]. Finally, a solid solution of Fe-Mn binary alloy with fcc crystal lattice was created with the thermodynamic data in the FSstel database [8].

Since MnO is more stable than FeO, the dissociation oxygen partial pressure of MnO is lower than that of FeO. Below the dissociation oxygen partial pressure of MnO, Fe and Mn form a solid solution. Above the dissociation oxygen partial pressure of MnO, $(\text{Mn}_{1-x}\text{Fe}_x)\text{O}$ mixed oxide is formed and the concentration of Fe dissolved in the $(\text{Mn}_{1-x}\text{Fe}_x)\text{O}$ increases with the ambient oxygen partial pressure. Above the dissociation oxygen partial pressure of FeO the entire alloy phase will oxidize and hence the concentration of Fe in $(\text{Mn}_{1-x}\text{Fe}_x)\text{O}$ is constant. The dissociation oxygen partial pressure of both MnO and FeO increases

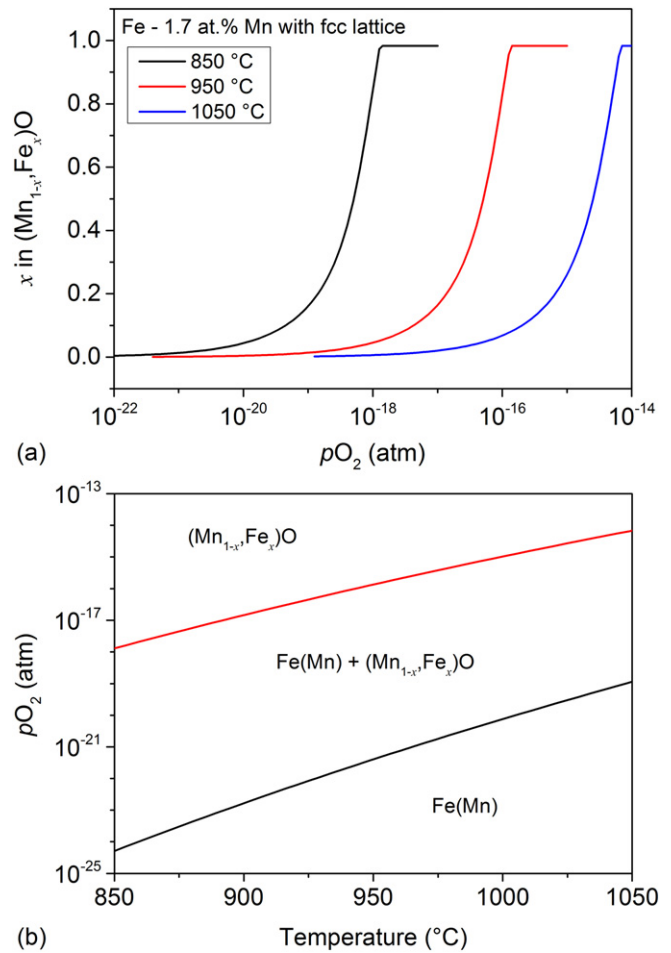


Fig. 1. (a) Computed Fe concentration in $(\text{Mn}_{1-x}\text{Fe}_x)\text{O}$ mixed oxide as a function of oxygen partial pressure (logarithm scale) at 850, 950 and 1050 °C in the Fe-Mn alloys with fcc crystal lattice at thermodynamic equilibrium with oxidizing gas atmosphere; (b) computed phase diagram of Fe - 1.7 at.% Mn alloy with fcc crystal lattice in oxidizing gas atmosphere, black and red lines represent the dissociation oxygen partial pressure of MnO and FeO, respectively.

with temperature; see Fig. 1(b). Between the dissociation oxygen partial pressures of MnO and FeO, the concentration of Fe in the $(\text{Mn}_{1-x}\text{Fe}_x)\text{O}$ decreases with temperature. Increasing Mn concentration in the Fe-Mn alloy from 1.0 to 2.5 at.% has a negligible effect on the Fe concentration in $(\text{Mn}_{1-x}\text{Fe}_x)\text{O}$. Also, the Fe concentration in $(\text{Mn}_{1-x}\text{Fe}_x)\text{O}$ is practically independent of the crystal lattice of the Fe-Mn alloy phase (i.e. ferrite or austenite).

The concentration depth profiles of dissolved oxygen in the IOZ of steels alloyed with 1.0, 1.7 and 2.5 at.% Mn after annealing at 950 °C in a gas mixture of N₂ plus 5 vol% H₂ with a dew point of 10 °C were calculated using a finite difference method considering the precipitation of oxides [2]. At 950 °C the mole fraction of dissolved oxygen at steel surface in equilibrium with the gas mixture of N₂ plus 5 vol% H₂ with a dew point of 10 °C is about 3.6×10^{-6} [7]. For the diffusion coefficient of oxygen a value of $3.5 \times 10^{-7} \text{ cm}^2/\text{s}$ [14] was adopted. As can be seen in Fig. 2(a), the concentration of dissolved oxygen decreases almost linearly with depth. The concentration of dissolved oxygen at internal oxidation front is practically zero. Since the depth of IOZ decreases with the bulk Mn concentration in the alloy, the concentration gradient of dissolved oxygen across the IOZ increases with the Mn concentration in the base alloy under the same ambient oxygen partial pressure.

Yet, the composition depth profile of $(\text{Mn}_{1-x}\text{Fe}_x)\text{O}$ internal precipitates can be calculated using the thermodynamic tool [9] considering local thermodynamic equilibrium with the dissolved oxygen. To this

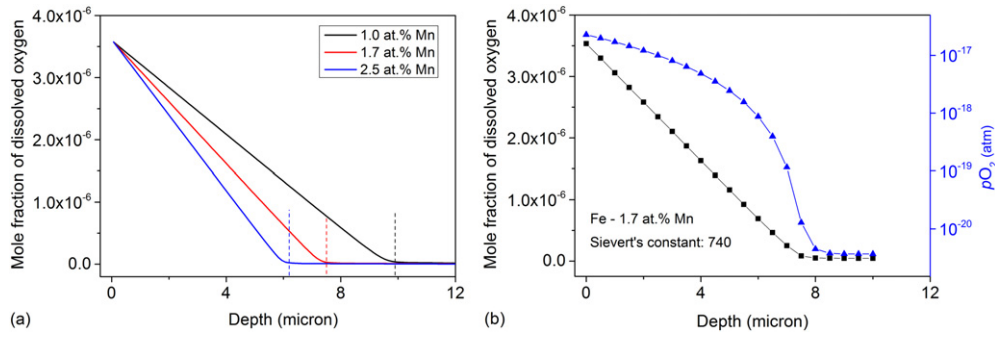


Fig. 2. (a) Simulated concentration depth profiles of dissolved oxygen in steel alloyed with 1.0, 1.7 and 2.5 at.% Mn, respectively, after annealing at 950 °C for 1 h in $N_2 + 5 \text{ vol}\% H_2$ gas mixture with dew point of 10 °C, dashed lines indicate the internal oxidation front where the concentration of oxide precipitate is almost zero. (b) The corresponding oxygen activity depth profile expressed as oxygen partial pressure (logarithm scale) for the 1.7 at.% Mn alloyed steel.

end, the activity of dissolved oxygen is expressed in terms of the oxygen partial pressure (pO_2 in atm) using Sievert's law [15]:

$$pO_2 = \left(\frac{N_O}{Ks} \right)^2, \quad (1)$$

where Ks is the Sievert's constant, N_O is the mole fraction of dissolved oxygen. The value of Ks for oxygen dissolution in iron is 739 at 950 °C [14]. Thus, the activity depth profile of dissolved oxygen in IOZ of the annealed Mn alloyed steels is obtained; see Fig. 2(b). Next, the concentration of Fe dissolved in the $(Mn_{1-x}Fe_x)O$ precipitates as a function of depth is determined from the composition diagram for $(Mn_{1-x}Fe_x)O$; see Fig. 1(a). It is predicted that the concentration of Fe in the internal $(Mn_{1-x}Fe_x)O$ precipitates decreases continuously with depth until the Fe concentration in $(Mn_{1-x}Fe_x)O$ becomes zero near internal oxidation front; see Fig. 3. The Fe concentration in the $(Mn_{1-x}Fe_x)O$ at steel surface is independent of bulk Mn concentration in steel; see Fig. 3. However, the concentration gradient of Fe in the $(Mn_{1-x}Fe_x)O$ precipitates increases with the bulk Mn concentration in the alloy, because the concentration gradient of dissolved oxygen increases with the bulk Mn concentration.

The observed extent of the IOZ of the steel alloyed with 1.7 at.% Mn after annealing at 950 °C for 1 h in N_2 plus 5 vol% H_2 with a dew point of 10 °C is about 8.7 μm ; see Fig. 4(a). The lattice constant derived from XRD measurements of the internal $(Mn_{1-x}Fe_x)O$ precipitates in the

annealed steel alloyed with 1.7 at.% Mn increases with depth. The lattice constants of the α -Fe matrix at different depths (about 2.867 Å) are close to the reported values of the α -Fe lattice constant, i.e. 2.866 [16], 2.865 [17] and 2.868 Å [18]. Thus the effect of any hydrostatic stress, if present, on $(Mn_{1-x}Fe_x)O$ precipitates is negligible. An in-plane residual stress in the $(Mn_{1-x}Fe_x)O$ precipitates and the α -Fe matrix of the annealed 1.7 at.% Mn alloyed steel was not observed. The deviation from stoichiometry, Δ in $Mn_{1-\Delta}O$, is small and thus can be neglected. The equilibrium value of Δ in $Mn_{1-\Delta}O$ at 950 °C is below 0.001 below an oxygen partial pressure of 3×10^{-17} [19] (which corresponds to a dew point of 12 °C in a gas mixture of N_2 with 5 vol% H_2). This value of Δ in $(Mn_{1-x}Fe_x)_{1-\Delta}O$ increases with Fe concentration and oxygen partial pressure [6]. However, below an oxygen partial pressure of 3×10^{-17} the equilibrium value of Δ in $(Mn_{1-x}Fe_x)_{1-\Delta}O$ computed with thermodynamic tool [8,9] is below 0.0025 at 950 °C. Hence, the influence of cation deficiency on the lattice constant of $(Mn_{1-x}Fe_x)O$ precipitates is negligible. Therefore, the change in the lattice constant of $(Mn_{1-x}Fe_x)O$ precipitates in the annealed 1.7 at.% Mn alloyed steel is solely attributed to the change in their composition as function of depth below the surface. The adopted lattice constant of pure MnO is 4.444 Å [7]. The lattice constant of $Fe_{1-\Delta}O$ increases from about 4.28 to 4.31 Å with $1-\Delta$ increasing from about 0.89 to 0.95 [20]. The extrapolated lattice constant for stoichiometric FeO equals about 4.334 Å [20]. The concentration of Fe in the $(Mn_{1-x}Fe_x)O$ was then determined by linear interpolation of the measured lattice constant, i.e. adopting Vegard's law [21]. Since the lattice constant of $(Mn_{1-x}Fe_x)O$ determined with XRD reflects an average value over a certain range of depth below the surface, its value is assigned to the analysis depth of 1.3 μm below the surface; cf. Section Experimental. The thus obtained composition depth profile of the $(Mn_{1-x}Fe_x)O$ internal precipitates in the annealed 1.7 at.% Mn alloyed steel is shown in Fig. 4(b).

As can be seen in Fig. 1(a), the level of the oxygen partial pressure in the annealing atmosphere may strongly affect the composition depth profile of internal $(Mn_{1-x}Fe_x)O$. For example, a slight increase in oxygen partial pressure from 2.3×10^{-17} (corresponding to the oxygen partial pressure level at 950 °C in $N_2 + 5 \text{ vol}\% H_2$ gas mixture with dew point of 10 °C) to 3.0×10^{-17} (corresponding to the oxygen partial pressure level at 950 °C in $N_2 + 5 \text{ vol}\% H_2$ gas mixture with dew point of 12 °C) increases the Fe concentration in the $(Mn_{1-x}Fe_x)O$ from x of 0.28 to 0.34. Hence, a slight increase of the annealing dew point can significantly increase the Fe concentration in the internal $(Mn_{1-x}Fe_x)O$ precipitates; see Fig. 4(b). Considering that the cooling from the annealing temperature is fast (about 180 °C/min), the composition of the oxide precipitates is likely preserved. The experimentally determined profile of Fe concentration in the internal $(Mn_{1-x}Fe_x)O$ of the annealed 1.7 at.% Mn alloyed steel fits perfectly to the profile predicted for a dew point of 12 °C rather than 10 °C; see Fig. 4(b). Since this difference in dew point is within the experimental error of about 2 °C (cf. Section Experimental), it can be concluded that local thermodynamic

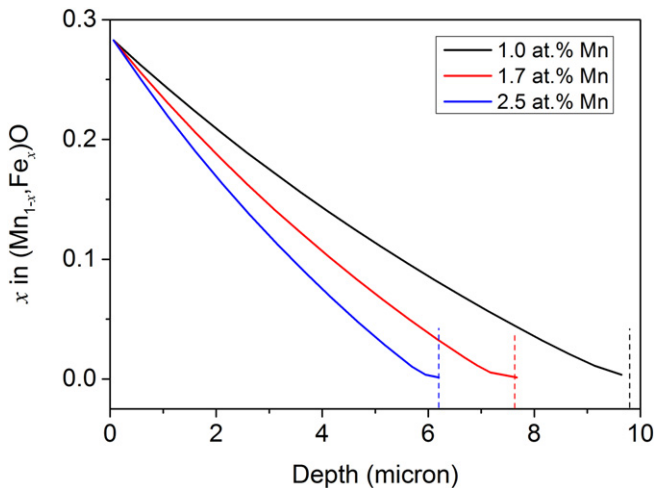


Fig. 3. Predicted depth profiles of Fe concentration in internal $(Mn_{1-x}Fe_x)O$ precipitates formed after annealing the 1.0, 1.7 and 2.5 at.% Mn alloyed steels at 950 °C for 1 h in $N_2 + 5 \text{ vol}\% H_2$ gas mixture with dew point of 10 °C; dashed lines indicate the internal oxidation front where the concentration of oxide precipitate is almost zero.

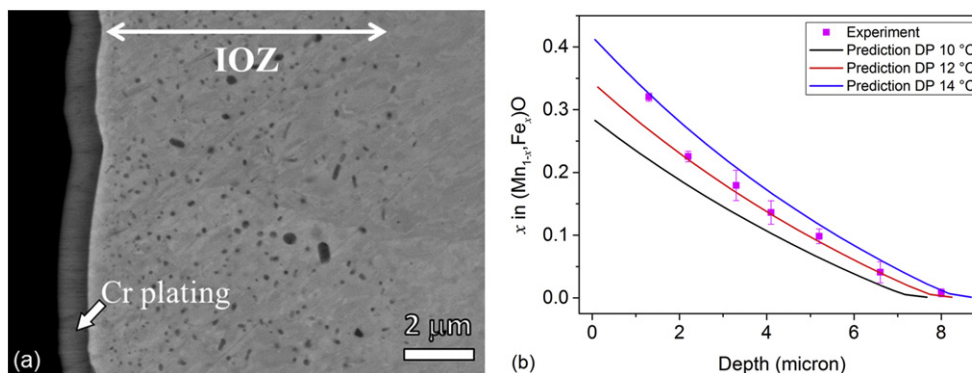


Fig. 4. (a) SEM image of internal oxidation zone (IOZ) of steel alloyed with 1.7 at.% Mn after annealing at 950 °C for 1 h in $\text{N}_2 + 5 \text{ vol}\% \text{H}_2$ gas mixture with dew point of 10 °C showing the oxide precipitates (dark spots in IOZ). (b) Predicted depth profiles of Fe concentration in the $(\text{Mn}_{1-x}\text{Fe}_x)\text{O}$ precipitates formed after annealing 1.7 at.% Mn alloyed steel at 950 °C for 1 h in $\text{N}_2 + 5 \text{ vol}\% \text{H}_2$ gas mixture with dew points (DP) of 10, 12 and 14 °C. The dots represent the experimentally determined Fe concentration in the $(\text{Mn}_{1-x}\text{Fe}_x)\text{O}$ precipitates formed after annealing 1.7 at.% Mn alloyed steel at 950 °C for 1 h in $\text{N}_2 + 5 \text{ vol}\% \text{H}_2$ gas mixture with dew point of about 10 °C.

equilibrium is established between the dissolved oxygen and the oxide precipitates in the IOZ of the annealed Mn alloyed steel.

Hence, the composition of the $(\text{Mn}_{1-x}\text{Fe}_x)\text{O}$ precipitates in IOZ is determined by the activity of dissolved oxygen. Since the activity of dissolved oxygen decreases from the alloy surface towards the internal oxidation front, the composition of the $(\text{Mn}_{1-x}\text{Fe}_x)\text{O}$ precipitates changes accordingly; i.e. the concentration of Fe in the $(\text{Mn}_{1-x}\text{Fe}_x)\text{O}$ precipitates decreases as a function of depth below the surface. Therefore, it is anticipated that when oxidizing multi-element alloyed steels internally, the composition as well as the type of multiple oxide precipitates formed in the IOZ will change as a function of depth, depending on the local oxygen activities. For example, it has been observed that during internal oxidation of Ni–Al–Si alloy different types of oxides (i.e. spinels, SiO_2 , and Al_2O_3) are formed in the IOZ at different depths, and the sequence of those oxides formed with increasing depth is consistent with the increasing thermodynamic stability of those oxides [22].

In conclusion, local thermodynamic equilibrium is established in the internal oxidation zone of Mn alloyed steels during annealing in an oxidizing environment. After internal oxidation of Mn alloyed steels mixed oxide precipitates $(\text{Mn}_{1-x}\text{Fe}_x)\text{O}$ are formed even at oxygen partial pressures (dew points) in the gas ambient well below the dissociation oxygen partial pressure of Wüstite (FeO). The composition of these $(\text{Mn}_{1-x}\text{Fe}_x)\text{O}$ precipitates depends on the local activity of oxygen in the IOZ. Consequently, the concentration of Fe in the $(\text{Mn}_{1-x}\text{Fe}_x)\text{O}$ precipitates decreases similar to the oxygen activity within the IOZ as a function of depth below the steel surface.

Acknowledgements

This research was carried out under project number M22.3.11439 in the framework of the research program of the Materials innovation institute (M2i). Financial support from International Zinc Association (IZA) for program ZCO-62 is gratefully acknowledged. The authors are indebted to Dr. W. Melfo of Tata Steel (Ijmuiden, The Netherlands) for

providing the Mn alloyed steel and the composition analysis. The authors thank Ing. J.C. Brouwer and Ing. C. Kwakernaak for technical support and assistance with experiments, and Ing. Ruud Hendrikx for the XRD measurements and analysis.

Appendix A. Supplementary data

Supplementary data to this article can be found online at <http://dx.doi.org/10.1016/j.scriptamat.2017.03.009>.

References

- [1] G.M. Song, T. Vystavel, N. van der Pers, J.T.M. De Hosson, W.G. Sloof, *Acta Mater.* 60 (2012) 2973.
- [2] V.A. Lashgari, G. Zimbitas, C. Kwakernaak, W.G. Sloof, *Oxid. Met.* 82 (2014) 249.
- [3] D. Huin, P. Flauder, J.B. Leblond, *Oxid. Met.* 64 (2005) 131.
- [4] J.B. Brunac, D. Huin, J.B. Leblond, *Oxid. Met.* 73 (2010) 565.
- [5] G. Zimbitas, W.G. Sloof, *Mat. Sci. Forum* 696 (2011) 82.
- [6] P. Franke, R. Dieckmann, *J. Phys. Chem. Solids* 51 (1990) 49.
- [7] V.A. Lashgari, Delft University of Technology, 2014, (Ph.D. thesis).
- [8] Factsage Database Documentation, <http://www.crct.polymtl.ca/fact/documentation/>.
- [9] C. Bale, P. Chartrand, S.A. Degterov, G. Eriksson, K. Hack, R. Ben Mahfoud, J. Melancon, A.D. Pelton, S. Petersen, *Calphad* 26 (2002) 189.
- [10] V.A. Lashgari, C. Kwakernaak, W.G. Sloof, *Oxid. Met.* 81 (2014) 435.
- [11] B.D. Cullity, S.R. Stock, *Elements of X-ray Diffraction*, third ed. Prentice Hall, New York, 2001.
- [12] W.A. Rachinger, *J. Sci. Instrum.* 25 (1948) 254.
- [13] NIST, SRM 660a, Gaithersburg, 2000.
- [14] J.H. Swisher, E.T. Turkdogan, *Trans. Metall. Soc. AIME* 239 (1967) 426.
- [15] D. Young, *High Temperature Oxidation and Corrosion of Metals*, Elsevier, Oxford, 2008.
- [16] Powder Diffraction File 00-006-0696.
- [17] Powder Diffraction File 04-007-9753.
- [18] Powder Diffraction File 04-014-0360.
- [19] M. Keller, R. Dieckmann, *Ber. Bunsenges. Phys. Chem.* 89 (1985) 883.
- [20] C. Haavik, S. Stolen, M. Hanfland, C.R.A. Catlow, *Phys. Chem. Chem. Phys.* 2 (2000) 5333.
- [21] L. Vegard, *Z. Phys.* 5 (1921) 17.
- [22] H.C. Yi, S.Q. Shi, W.W. Smeltzer, A. Petric, *Oxid. Met.* 43 (1995) 115.